Analysis of Bridge Time-dependent Performance Based on Dynamic Bayesian Networks

BUYU JIA, XIAOLIN YU, QUANSHENG YAN AND ZHENG YANG

School of Civil Engineering and Transportation, South China University of Technology, Guangzhou 510640, China

Email: *ctjby@scut.edu.cn, xlyu1@scut.edu.cn*

Abstract: Current analysis of bridge time-dependent performance is mostly based on present test data or certain single approximate computational formulas. Thus, it is usually unable to combine prior knowledge of bridge time-dependent performances with on-site detection information effectively, and the evaluation model or parameters could not be updated on time. On the basis of the bridge characteristic during the time varying process, the Dynamic Bayesian Network (DBN), which could effectively assess bridge time-dependent performance, is proposed in this study. Two bridges, the performance of which is changed by internal and external environments, are taken as research objects. DBN is used to approximate the model of time-dependent performance of two bridges. Model updating is also realized by utilizing detection information. Results validate the feasibility and effectiveness of the proposed method.

Keywords: bridge, time-dependent performance, Dynamic Bayesian Networks, detection information, model updating

1. Introduction

In recent years, researchers have made numerous achievements in the field of bridge time-dependent performance and developed methods, such as the accelerated test method, grey system-based theory, artificial neural networks, and Markov chain method. The accelerated test method (Li, 2003) is a process in which the artificial acceleration process in the lab is applied to imitate the performance degradation process. The inherent error of mathematical relation exists in two different degradations. Thus, the predicted results sometimes might not be reasonable. The determinable mathematical model (Gode, 2014) applies certain deterministic mathematical models to simulate time-dependent performance. The deterministic model has the following disadvantages: some random uncertain factors are often ignored, and it is inconvenient to revise the original model when a new detection date is gained or a new system is adopted. The grey system-based theory (Jia and Chen, 2009; Liang et al., 2002) is a time series method, which is unsuitable for making predictions in case of strong randomness and long-term periods. Artificial neural networks (Hasancebi and Dumlupinar, 2013; Huang, 2010) are extensively used in the prediction of bridge structure degradation. However, artificial neural networks do not have certain clear rules to follow and are sometimes unstable. The Markov chain method (Wellalage et al., 2015; Li et al., 2014; Bocchini et al., 2013) is the most widely used technique and approximates structure degradation by using transferring probability from one state to another. In the well-known American PONTIS (Thompson, 1993) and BRIDGIT (Hawk, 1995)

systems, the Markov chain method is taken as a basis of theory when predicting bridge time-dependent performance.

An important problem in the assessment of a bridge structure performance is that many existing methods or models depend on certain formulas only. Therefore, they could not update existing methods or models by detection information and could not comprehensively utilize the existing universal rule of structural degradation and test information. Dynamic Bayesian networks (DBN) (Murphy, 2002) are based on Bayesian theory, which could not only deal with time series data and complex structural problems, but also update the model on time by using detection information. In recent years, DBN has been applied and developed in many fields, such as state identification (Popa et al., 2010) and video analysis (Swears et al., 2010). However, its research and extension is limited in the structural engineering field and focuses mainly on static Bayesian networks. Faber et al. (2002) assessed the risk of a concrete offshore platform's decommissioning by using Bayesian probability networks. He mainly used Bayesian probability networks to perform a sensibility analysis and improve the risk model. Langseth and Portinale (2007) established a computing framework that used Bayesian networks to perform the structural reliability analysis. Attoh and Bowers (2006) determined that Bayesian networks are more suitable than the fault tree method for demonstrating the bridge degradation process.

DBN is applied to the assessment of bridge time-dependent performance in this study. The DBN model is established and could effectively describe the time-

such as Markov chain Monte Carlo algorithms (Doucet et al., 2000) and particle filtering (Arulampalam et al., 2002). The deterministic algorithm is restricted by its finite DBN topological structure, which is not practical. The MCMC algorithm has strong applicability, but its computing efficiency could not be guaranteed. The particle filtering algorithm is suitable for online processing, but it lacks precision. Exact inference algorithms include forward-backward algorithm (Murphy, 2002), interface algorithm (Murphy, 2002), and frontier algorithm (Langseth and Bangso, 2001).

When the conditional probability distributions (CPD) of all random variables are linear Gaussian, the DBN can be decomposed and transformed into KFM. The forward-backward algorithm based on the Kalman smoother (Murphy, 2002), which is the one of exact inference algorithms, is applied to the inference in this study; see Appendix for details.

5. Assessment of bridge time-dependent performance by considering the change of internal environment

A simply-supported reinforced concrete T-shaped beam bridge built in 1966 is considered in this paper. This bridge has a total of six spans that are 15 m long each. Figure 3 shows the cross section of a T-shaped beam.

The structural performance degradation caused only by the reduced structural resistance is considered, while the time-dependent load is disregarded. As for the reinforced concrete structure, two major factors influence the structural performance degradation, namely, reinforcing bar corrosion and reinforcement bar strength degradation (the degradation of bonding behavior between the reinforcement bar and concrete is not considered in this paper).
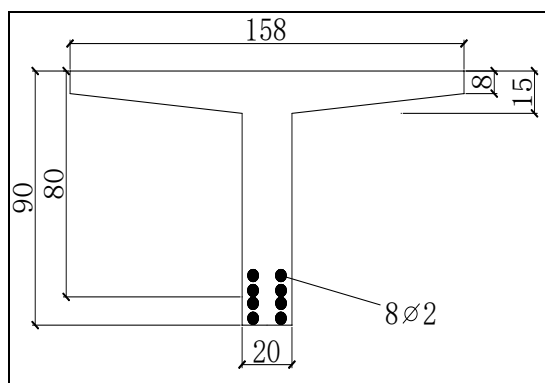

Fig. 3: T-beam cross section (unit: cm)

The time-varying regularity of the two factors and some priori formulas are given as follows:

(1) **Reinforcing steel corrosion.** Only the reinforcing steel corrosion caused by chloride erosion is considered. First, with the use of Fick's second law, the corrosion's starting time is obtained as

$$T_i = \frac{c^2}{4D_c}\left[\text{erf}^{-1}\left(\frac{Cl_s - Cl_{cr}}{Cl_s - Cl_0}\right)\right]^{-2} , \qquad (3)$$

where c is the cover thickness, D_c is the chloride diffusion coefficient, Cl_{cr} is the critical chloride concentration, Cl_0 is the initial chloride concentration, and Cl_s is the surface chloride concentration.

The rate of corrosion after corrosion at time t is subsequently given as (Vu and Stewart, 2000)

$$i_{corr}(t) = i_{corr} \times 0.85(t - T_i)^{-0.29} , \qquad (4)$$

where $i_{corr} = 37.8(1 - 27/(f_c + 13.5))^{-1.64}/c$, and f_c is the compressive strength of concrete.

Considering the uniform corrosion, the diameter of the corroded reinforcement bar at time t can be obtained as (Stewart and Rosowsky, 1998)

$$D(t) = D_0 - 0.0232(t - T_i)i_{corr}(t) , \qquad (5)$$

where D_0 is the initial diameter of the reinforcement bar.

(2) **Degradation of reinforcement bar strength.** The strength degradation of concrete has minimal influence on the structural performance. Thus, its influence is ignored. The relation between the yield strength of the reinforcement bar and the loss of cross-sectional area of the corroded reinforcement bar is shown as follows:

$$f_y(t) = \left[1 - \alpha_y \frac{A_p(t)}{A}\right]f_{y0} , \qquad (6)$$

where f_{y0} is the yield strength of the reinforcement bar before corrosion, $f_y(t)$ is the yield strength of the corroded reinforcement bar at time t, α_y is an impact factor, and $A_p(t)$ is the loss of the cross-sectional area of the corroded reinforcement bar at time t.

(3) **Resistance of reinforcement concrete structure after corrosion.** The flexural capacity of the reinforced concrete beam after corrosion can be written as

$$\begin{cases} M(t) = k_b \alpha_1 f_c bx(h_0 - 0.5x) \\ x = A(t)f_y(t)/(\alpha_1 f_c b) \end{cases} \qquad (7)$$

where $M(t)$ is the flexural capacity of the reinforced concrete beam, k_b is the model uncertainty factor, b is the width of the section, h_0 is effective depth of the section, α_1 is the stress-block factor for concrete, and $A(t)$ is the section area of tensile reinforcement after corrosion, which can be obtained by using Eq. (5).

The compressed corroded reinforcement is not considered.

Eqs. (3)–(7) are prior knowledge obtained from previous degradation rules of bridge time-dependent performance. Prior knowledge does not seem to be working well at all times in practical projects. In the following paragraphs, prior knowledge achieved from Eqs. (3)–(7) and detection information will be combined by the DBN model and will be revised by updating the DBN model.

Major parameters involved in Eqs. (3)–(7) are considered variable nodes in DBN. The statistical characteristics of variables are given in Table 1.

Table 1: Statistical characteristics of variables (example 1)

Variable	Mean	Variation coefficient
surface chloride concentration $\mathbf{Cl_s}$/(kg/m^3)	39.200	0.160
critical chloride concentration $\mathbf{Cl_{cr}}$/(kg/m^3)	11.025	0.160
initial chloride concentration $\mathbf{Cl_0}$/(kg/m^3)	0.735	0.100
chloride diffusion coefficient $\mathbf{D_c}$/(cm^2/a)	23.360	0.310
compressive strength of concrete $\mathbf{f_c}$/Mpa	27.800	0.110
cover thickness $\mathbf{c}$/mm	30.500	0.050
initial diameter of reinforcement bar $\mathbf{D_0}$/mm	20.000	0.025
yield strength of reinforcement bar before corrosion $\mathbf{f_{y0}}$/Mpa	303.300	1.014×10^{-1}

The limit value of flexural capacity is set as $M_c = 300 kN\Box m$. The corresponding limit state function (LSF) can then be written as

$$g = M_c - M(t) \ . \qquad (8)$$

The LSF is expressed as variable E in the DBN model. $E \leq 0$ and $E > 0$ indicate failure and safety, respectively.

The corresponding DBN model is shown in Figure 4. The transition matrices of time invariant variables, such as $Cl_{s(t)} \rightarrow Cl_{s(t+1)}$, $Cl_{cr(t)} \rightarrow Cl_{cr(t+1)}$, $Cl_{0(t)} \rightarrow Cl_{0(t+1)}$, $D_{c(t)} \rightarrow D_{c(t+1)}$, $f_{c(t)} \rightarrow f_{c(t+1)}$, $c_{(t)} \rightarrow c_{(t+1)}$, $D_{0(t)} \rightarrow D_{0(t+1)}$, and $f_{y0(t)} \rightarrow f_{y0(t+1)}$, are diagonal unit matrices. The CPDs between other nodes are obtained by using Monte Carlo simulation and parameter learning method.

The time interval is supposed to be $\Delta t = 1$ year, and the total lasting time is $T = 80$. A detection result was obtained in 2006, which is $b_{40} = 456 kN\Box m$. Through the parameter learning method based on the EM algorithm and the inference based on the

forward–backward algorithm, the original and updated results of the flexural capacity M are shown in Figure 5.

Figure 5 shows that the DBN model can effectively approximate the degradation process of sectional flexural capacity caused by reinforcement steel corrosion and fully exhibits the information updating ability of DBN. The detection information seems to be 'bad' evidence because the updated assessment of flexural capacity has a certain decrease. Results indicate that prior experience or theoretical equation could not be applied in all cases. The on-site information of the existing bridge should be considered. In other words, prior knowledge of the bridge time-dependent performance and detection information should be combined and fully used.

With the addition of functional variable E into the network, a reliability analysis based on the Monte Carlo simulation method was conducted, and the excellent expandability of DBN was demonstrated. Figure 6 shows the comparison results of reliability between the original and updated models, and indicates that the reliability value has changed, with the updated reliability being smaller than the original one.

DBN can also update the original distribution of the node variable by model inference. Figure 7 provides the original and updated results of the probability density function (PDF) of some variables when $t = 30$. After the updating, the means of compressive strength of concrete (f_c), initial diameter of reinforcement bar (D_0), and yield strength of reinforcement bar before corrosion (f_{y0}) were reduced. Their standard deviations were also decreased considerably. If a more observed date is achieved, then the probability distribution will be more realistic. Another detection result was obtained in 2011, which is $b_{45} = 441 kN\Box m$. The twice-updated results (also at $t = 30$) are shown in Figure 8. After the second updating, the means of f_c and D_0 increased and were even greater than the original results, whereas the mean of f_{y0} decreased further. Remarkably, all standard deviations of the three variables decreased further, thereby indicating that the accumulated detection information will be helpful in preventing the discrete degree of variables from decreasing.

6. Assessment of bridge time-dependent performance by considering the change of external environment

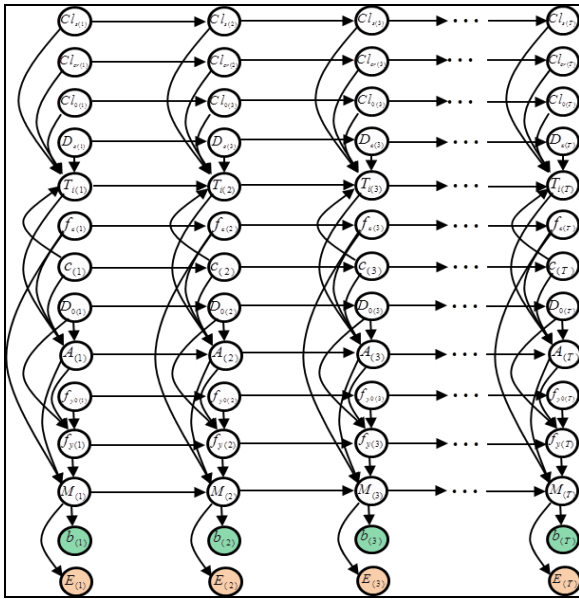A large cantilever prestressed concrete box beam bridge is selected to apply the introduced method.

Fig. 4: *DBN model of example 1 (influence of internal environment on bridge time-dependent performance).*
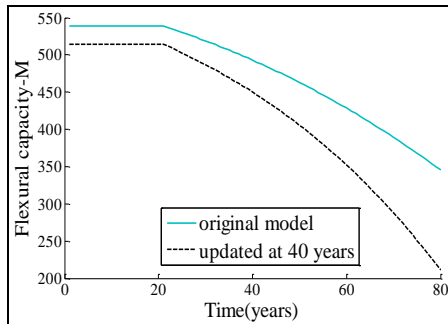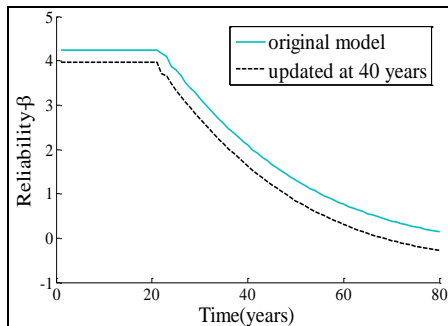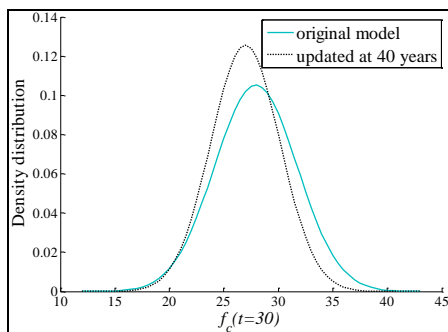

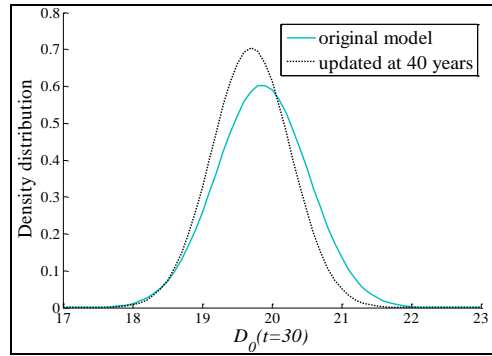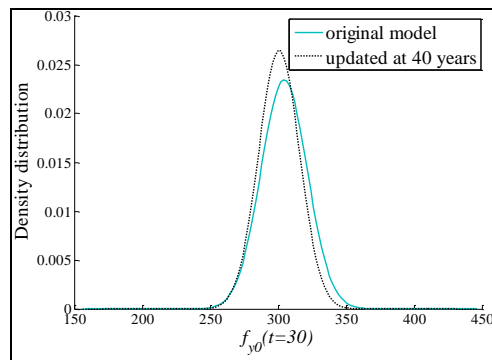**Fig. 5:** *Updating of the flexural capacity.*

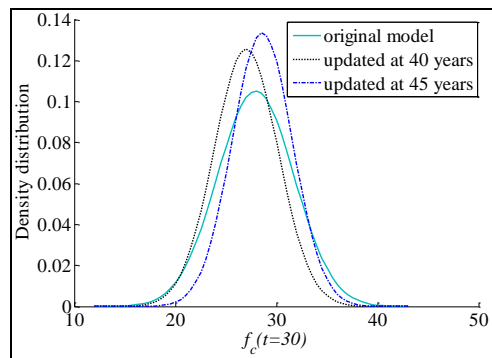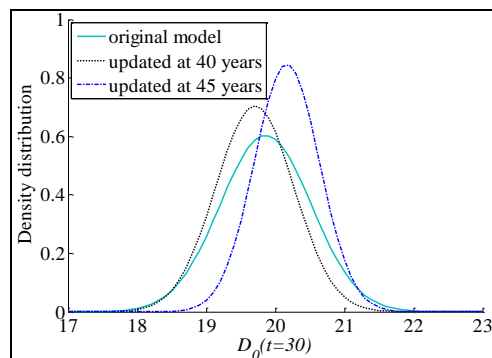**Fig. 6:** *Updating of the reliability.*
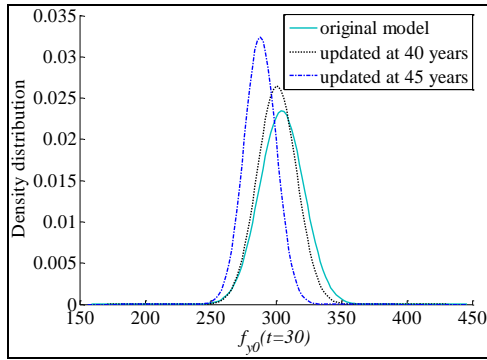

(a) f_c

(b) D_0

(c) f_{y0}

Fig. 7: *Updating of the distributions of* $f_c(t=30)$、$D_0(t=30)$、$f_{y0}(t=30)$ *with first detection results (* $b_{40}=456kN\cdot m$ *).*

(a) f_c

(b) D_0

(c) f_{y0}

Fig. 8: *Updating of the distributions of* $f_c(t=30)$、$D_0(t=30)$、$f_{y0}(t=30)$ *with two-times detection results* ($b_{40}=456kN\square m$ $b_{45}=441kN\square m$).

6. Assessment of bridge time-dependent performance by considering the change of external environment

A large cantilever prestressed concrete box beam bridge is selected to apply the introduced method. The spans of the bridge beam are 4×42 m long and 33.5 m wide. Each cantilever is 7.174 m long and 0.25 m thick. The bottom plate is 0.175 m wide and 0.25 m thick. The cross section of the bridge is shown in Figure 9.
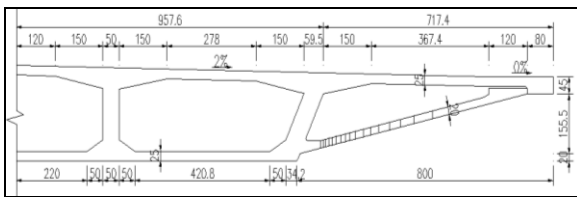

Fig. 9: *Half of cross section (unit: cm).*

In view of the transverse cracked problem of concrete in the root of the large cantilever, the time-varying transverse stress in the root of cantilever of mid-span caused by the external environment is studied. The live load, negative temperature gradient, and shrinkage are set as the main variables of the external environment.

(1) **Live load.** The time-varying live load in the future is predicted based on a statistical report (2013) on the growth rate of local traffic. For convenience of expression, the live load is replaced by a live load ratio, which is the predicted value divided by the load standard value in the *Chinese General Code for Design of Highway Bridges and Culverts* (2004). After fitting, the live load ratio at time t is given as

$$F(t)=\lambda_1 e^{-((t-a_1)/a_2)^2}+\lambda_2 e^{-((t-a_3)/a_4)^2},\qquad(9)$$

where λ_1, a_1, a_2, λ_2, a_3, and a_4 are fitting parameters.

2) **Max temperature difference in the negative temperature gradient.** According to the local climate feature, the annual max temperature difference is supposed to be stable, and the max temperature difference is considered a time-invariant variable

$$T_g(t)=-4.\qquad(10)$$

(3) **Shrinkage strain**. With the shrinkage strain equation in the *Code for design of highway reinforced concrete and prestressed concrete bridges and culverts* (2004) combined with the actual structure of the bridge, the shrinkage strain at time t is fitted as

$$S(t)=-\eta_1 e^{b_1 t}+\eta_2 e^{-b_2 t},\qquad(11)$$

where η_1, b_1, η_2, and b_2 are fitting parameters.

The max transverse stress value $\sigma(t)$ in the root of the cantilever is obtained by evaluating $F(t)$, $T_g(t)$, and $S(t)$ by using Eqs. (9)–(11) and implementing the structural computation by using the ANSYS software. Similar to Eqs. (3)–(7), Eqs. (9)–(11) are also prior knowledge obtained from the subjective prediction and specification by specialists. When they are used in actual situations, the results might not be reasonable.

In the following paragraphs, the actual detection information is utilized by updating the DBN model to revise prior knowledge. The major parameters involved in Eqs. (9)–(11) are set as variables in DBN. The statistical characteristics of variables are given in Table 2, while the corresponding DBN model is shown in Figure 10.

Table 2: *Statistical characteristics of variables (example 2)*

Variable	Mean	Variation coefficient
λ_1	3.305	0.100
a_1	67.860	0.050
a_2	54.290	0.050
λ_2	5.118×10^{-1}	0.100
a_3	11.770	0.050
a_4	10.680	0.050
η_1	19.120	0.060
b_1	1.423×10^{-2}	0.020
η_2	14.480	0.060
b_2	2.278×10^{-1}	0.020
T_g	-4.000	0.110

The time interval is supposed to be $\Delta t=1$ year, and the total lasting time is $T=20$. The detection result at $t=6$ is assumed as $b_6=-0.7MPa$. The original and updated results of the max transverse stress in the root of cantilever (σ) obtained by using the parameter

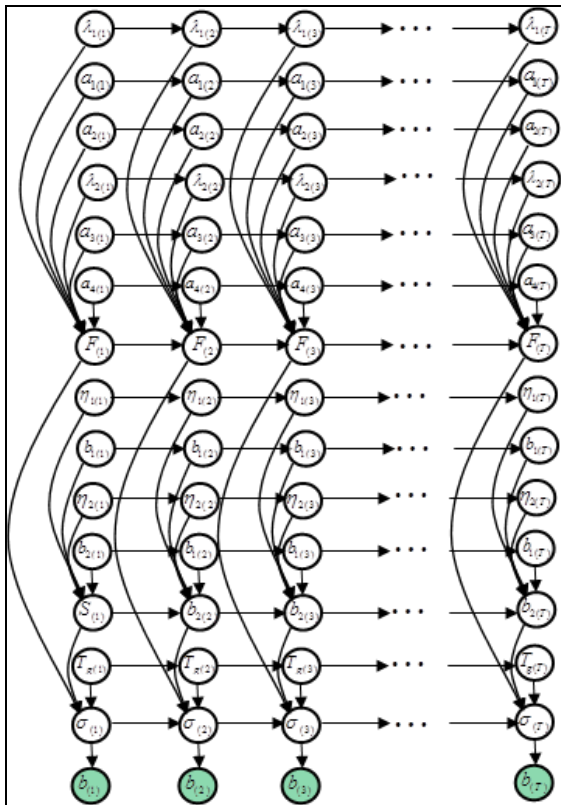learning and the inference methods are shown in Figure 11.

Fig. 10: *DBN model of example 2 (influence of external environment on bridge time-dependent performance).*
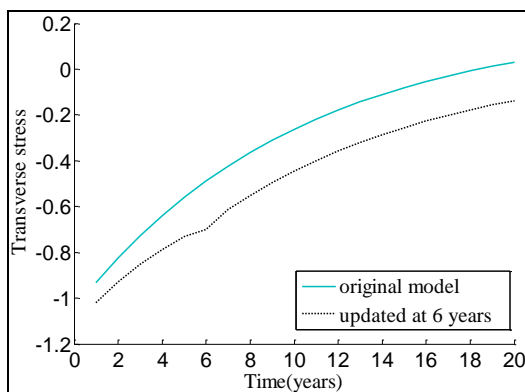

Fig. 11: *Updating of the transverse stress.*

Figure 11 shows that the DBN model has been applied successfully in the assessment of bridge time-dependent performance when the external environment change is considered. The DBN model can efficiently approximate the time-dependent process of transverse stress caused by live load action, negative temperature gradient, and shrinkage action. From the view of cracking resistance, $b_6 = -0.7\text{MPa}$ seems to be 'good' evidence, because the updated transverse compressive stress is greater than the original one.

Figure 12 shows the original and updated results of the PDF of the live load ratio variable F, max temperature difference T_g, and shrinkage stress variable S, which are evaluated at $t = 4$. The figure indicates that the probability distribution of each node variable changed after updating. The live load ratio has the highest sensibility, in which both mean and standard deviation reduced considerably. Although the sensibility of the shrinkage strain and max temperature difference is smaller than that of the live load ratio, both are affected by the detection information, and their means are lower than the original ones.

Another detection result at $t = 12$ is considered, in which $b_{12} = -0.5\text{MPa}$. Figure 13 shows the twice-updated PDF results of F, T_g, and S, which are evaluated at $t = 10$. The figure indicates that all the means (absolute value) of F, S, and T_g after the second update decrease further compared with the result that was updated for the first time, in which the decrease of F is the largest. The standard deviation of three values had different degrees of decrease (the standard deviation of T_g between the first update and the second update has little difference), which means that the discrete degree of the variable was reduced.
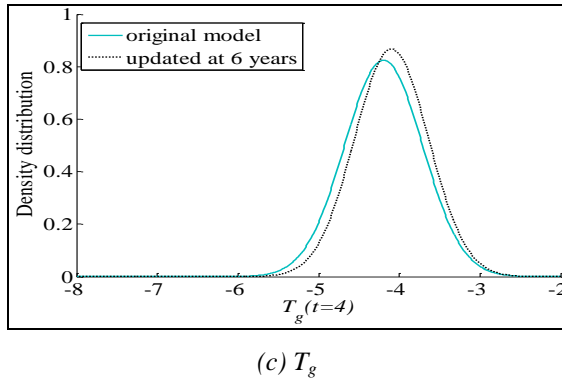

(a) S

(b) F

(c) T_g
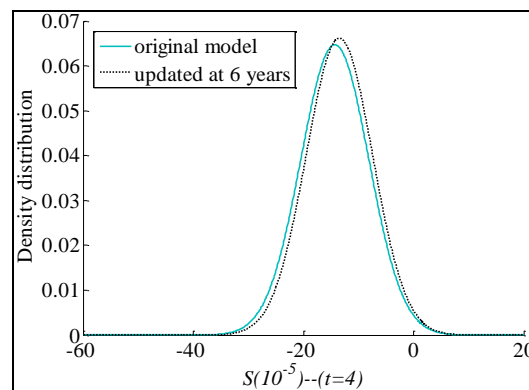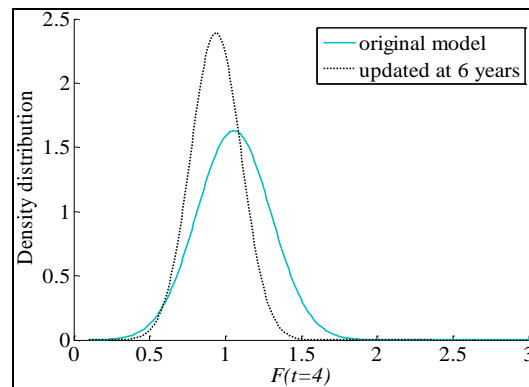
Fig. 12: *Updating of the distributions of $F(t=4)$, $T_g(t=4)$ and $S(t=4)$ with first detection results ($b_6 = -0.7\text{MPa}$)*
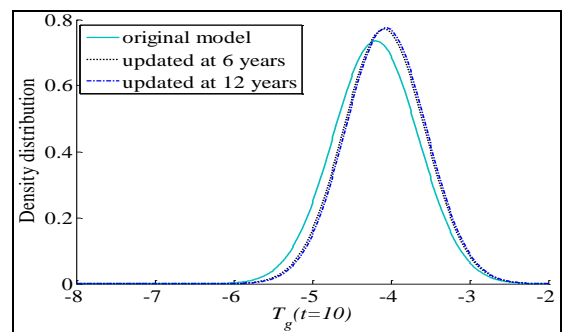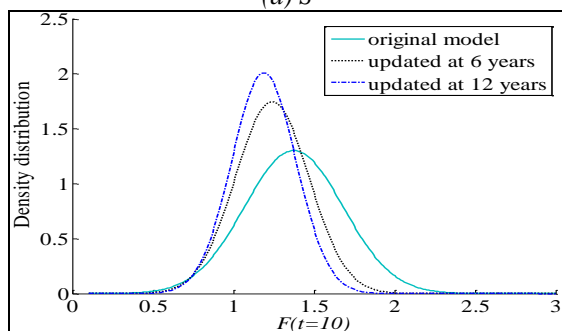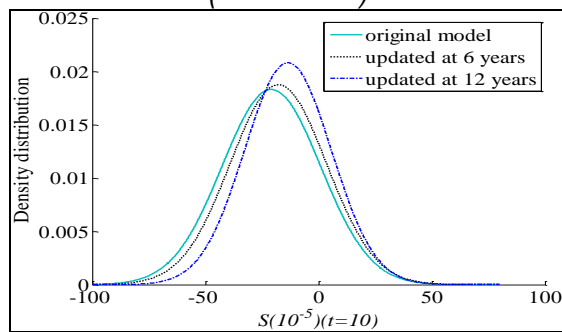

(a) S

(b) F

(c) T_g

Fig. 13: *Updating of the distributions of $F(t=10)$, $T_g(t=10)$ and $S(t=10)$ with two-times detection results ($b_6 = -0.7\text{MPa}$, $b_{12} = -0.5\text{MPa}$).*

7. Conclusions

This study analyzed bridge time-dependent performance. A series of methods for the application

of DBN to the assessment of bridge time-dependent performance was proposed. The main contributions of this study can be summarized as follows:

(1) DBN is taken as a complicated causal network combined with time series. DBN has unique advantages in dealing with time series data during the bridge time-dependent process and in describing multi-layer structures. This study suggests DBN as a tool to approximate the bridge time-dependent process and shows the application potential of DBN in the field of bridge structural analysis.

(2) A simply-supported reinforced concrete T-shape beam bridge influenced by the internal environment is taken as a research object. DNB is applied successfully to approximate the degradation process of sectional flexural capacity. A large cantilever prestressed concrete box beam bridge influenced by the external environment is taken as another object. The time-dependent process of transverse stress in the root of the cantilever caused by live load, shrinkage, and temperature difference in the negative temperature gradient is also realized successfully by DBN.

(3) The model updating of the two bridges is achieved by detection information. Calculation results show that DBN could make compound use of prior knowledge and on-site detection information. Detection information could also be used to update and revise the original model continuously. Meanwhile, the probability distribution of node variable can be updated through message passing among the nodes in DBN. The updating will be helpful to ensure the decrease of the discrete degree of variables.

(4) DBN also has a good ability to expand the network. In the case of the simply-supported reinforced concrete T-shape beam bridge, reliability computing is successfully realized by DBN, and the reliability is also updated because of the probability distribution of node variables has been updated.

8. Acknowledgments

9. Appendix

9.1. Parameter Learning

With $\mathbf{X}$ as a hidden variable and $\mathbf{Y}$ as an observed variable, the log-likelihood of observed data can be expressed as

$$L(\theta) = \log P(\mathbf{Y}|\theta) = \log \int_{\mathbf{X}} P(\mathbf{X}, \mathbf{Y}|\theta)d\mathbf{X}. \quad \text{(A.1)}$$

Using Jensen's inequality is the basic concept of the EM algorithm. For any concavity function f, the following inequality can be obtained by utilizing Jensen's inequality:

$$f\left(\sum_j \lambda_j y_j\right) \geq \sum_j \lambda_j f(y_j), \qquad (A.2)$$

where $\sum_j \lambda_j = 1$. The log-likelihood function is the concavity function; thus, according to Eq. (A.2), Eq. (A.1) can be rewritten as follows:

$$
\begin{aligned}
L(\theta) &= \log \int_X P(\mathbf{X}, \mathbf{Y}|\theta) d\mathbf{X} \\
&= \log \int_{\mathbf{X}} q(\mathbf{X}) \frac{P(\mathbf{X}, \mathbf{Y}|\theta)}{q(\mathbf{X})} d\mathbf{X} \\
&\geq \int_{\mathbf{X}} q(\mathbf{X}) \log \frac{P(\mathbf{X}, \mathbf{Y}|\theta)}{q(\mathbf{X})} d\mathbf{X} \\
&= \int_{\mathbf{X}} q(\mathbf{X}) \log P(\mathbf{X}, \mathbf{Y}|\theta) d\mathbf{X} - \int_{\mathbf{X}} q(\mathbf{X}) \log q(\mathbf{X}) d\mathbf{X} \\
&= H(q, \theta)
\end{aligned}
\qquad , (A.3)
$$

where q meets $\int_{\mathbf{X}} q(\mathbf{X}) d\mathbf{X} = 1$ and $0 \leq q(\mathbf{X}) \leq 1$.

$H(q,\theta)$ is maximized with respect to q and θ in turn. The two basic steps of the EM algorithm are

E-step: $\quad q_{k+1} = \arg\max_q H(q, \theta_k)$. $\qquad$ (A.4)

M-step: $\quad \theta_{k+1} = \arg\max_\theta H(q_{k+1}, \theta)$. $\qquad$ (A.5)

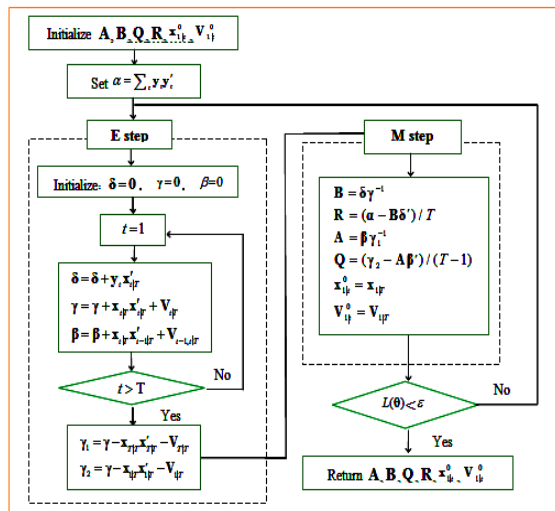The flowchart of the parameter learning of the linear Gaussian DBN is shown in Figure A.1.

Fig. A.1: *Flowchart of parameter learning of linear Gaussian DBN.*

9.2. Inferences

(1) Forwards pass

$(\mathbf{x}_{t|t}, \mathbf{V}_{t|t})$ is denoted as the mean and covariance of $P(\mathbf{X}_t|\mathbf{y}_{1:t})$. According to Eq. (2), the forward operator is defined as

$$(\mathbf{x}_{t|t}, \mathbf{V}_{t|t}, \mathbf{L}_t) = \mathrm{Fwd}(\mathbf{x}_{t-1|t-1}, \mathbf{V}_{t-1|t-1}, \mathbf{y}_t; \mathbf{A}_t, \mathbf{B}_t, \mathbf{Q}_t, \mathbf{R}_t). \quad (A.6)$$

First, the predicted mean and variance are calculated.

$$
\begin{cases}
\mathbf{x}_{t|t-1} = \mathbf{A}\mathbf{x}_{t-1|t-1} \\
\mathbf{V}_{t|t-1} = \mathbf{A}\mathbf{V}_{t-1|t-1}\mathbf{A}' + \mathbf{Q}
\end{cases}
. \qquad (A.7)
$$

The error in prediction, variance of the error, Kalman gain matrix, and conditional log-likelihood are then computed.

$$
\begin{cases}
\mathbf{e}_t = \mathbf{y}_t - \mathbf{B}\mathbf{x}_{t|t-1} \\
\mathbf{S}_t = \mathbf{B}\mathbf{V}_{t|t-1}\mathbf{B}' + \mathbf{R} \\
\mathbf{K}_t = \mathbf{V}_{t|t-1}\mathbf{B}'\mathbf{S}_t^{-1} \\
\mathbf{L}_t = \log N(\mathbf{e}_t; \mathbf{0}, \mathbf{S}_t)
\end{cases}
. \qquad (A.8)
$$

Finally, the mean and predicted value of variance are updated.

$$
\begin{cases}
\mathbf{x}_{t|t} = \mathbf{x}_{t|t-1} + \mathbf{K}_t\mathbf{e}_t \\
\mathbf{V}_{t|t} = (\mathbf{I} - \mathbf{K}_t\mathbf{B})\mathbf{V}_{t|t-1} = \mathbf{V}_{t|t-1} - \mathbf{K}_t\mathbf{S}_t\mathbf{K}_t'
\end{cases}
. \quad (A.9)
$$

(2) Backwards pass

The backward operator is defined as follows

$$(\mathbf{x}_{t|T}, \mathbf{V}_{t|T}, \mathbf{V}_{t-1,t|T}) = \mathrm{Back}(\mathbf{x}_{t+1|T}, \mathbf{V}_{t+1|T}, \mathbf{x}_{t|t}, \mathbf{V}_{t|t}; \mathbf{A}_{t+1}, \mathbf{Q}_{t+1}) \quad (A.10)$$

First, the predicted mean and variance are computed as before.

$$
\begin{cases}
\mathbf{x}_{t+1|t} = \mathbf{A}_{t+1}\mathbf{x}_{t|t} \\
\mathbf{V}_{t+1|t} = \mathbf{A}_{t+1}\mathbf{V}_{t|t}\mathbf{A}_{t+1}' + \mathbf{Q}_{t+1}
\end{cases}
. \qquad (A.11)
$$

The smoother gain matrix is then estimated.

$$\mathbf{J}_t = \mathbf{V}_{t|t}\mathbf{A}_{t+1}'\mathbf{V}_{t+1|t}^{-1}. \qquad (A.12)$$

Finally, the estimates of mean, variance, and cross variance $\mathbf{V}_{t-1,t|T} = \mathrm{Cov}[\mathbf{X}_{t-1}, \mathbf{X}_t|\mathbf{y}_{1:T}]$ are calculated.

$$
\begin{cases}
\mathbf{x}_{t|T} = \mathbf{x}_{t|t} + \mathbf{J}_t(\mathbf{x}_{t+1|T} - \mathbf{x}_{t+1|t}) \\
\mathbf{V}_{t|T} = \mathbf{V}_{t|t} + \mathbf{J}_t(\mathbf{V}_{t+1|T} - \mathbf{V}_{t+1|t})\mathbf{J}_t' \\
\mathbf{V}_{t-1,t|T} = \mathbf{J}_{t-1}\mathbf{V}_{t|T}
\end{cases}
. \qquad (A.13)
$$

References

[1] Li C. Q. (2003). "Life-cycle modeling of corrosion-affected concrete structures: Propagation", *Journal of Structural Engineering-ASCE*, 129(6), 753-761.

[2] Gode K. (2014). "Predicting the Service Life of Concrete Bridges Based on Quantitative Research", *Construction Science*, 15(1), 11-18.

[3] Jia C., Qu H., and Chen G. (2009). "Prediction of stress of concrete rigid frame bridge based on gray BP neural network", *Journal of China Three Gorges University*, 31(1), 56-59.

[4] Liang M. T., Chang J. W., and Li Q. (2002). "Grey and regression models predicting the remaining service life of existing reinforced concrete bridges", *Journal of Grey System*, 14(3), 291-310.

[5] Hasancebi O. and Dumlupinar T. (2013). "Linear and nonlinear model updating of reinforced concrete T-beam bridges using artificial neural networks", *Computers & Structures*, 119, 1-11.

[6] Huang Y. (2010). "Artificial neural network model of bridge deterioration", *Journal of Performance of Constructed Facilities*, 24(6), 597-602.

[7] Wellalage N. K. W., Zhang T., and Dwight R. (2015). "Calibrating Markov chain-based deterioration models for predicting future conditions of railway bridge elements", *Journal of Bridge Engineering*, 20(2), 1-13.

[8] Li L., Sun L., and Ning G. (2014). "Deterioration prediction of urban bridges on network level using Markov-chain model", *Mathematical Problems in Engineering*, 2014(728107).

[9] Bocchini P., Saydam D., and Frangopol D. M. (2013). "Efficient, accurate, and simple Markov chain model for the life-cycle analysis of bridge groups", *Structural Safety*, 40, 51-64.

[10] Thompson P. D. (1993). "Pontis bridge management system", *Proceedings of the ASCE 3rd International Conference on Applications of Advaced Technologies in Transportation Engineering*, 500-506.

[11] Hawk H. (1995). "BRIDGIT deterioration models", *Transportation Research Record*, 1995(1490), 19-22.

[12] Murphy K. P. (2002). "Dynamic Bayesian Networks Representation, Inference and Learning", Ph.D. Thesis, University of California, Berkeley, USA.

[13] Popa M. C, Rothkrantz L. J. M., Datcu D., Wiggers P., Braspenning R. and Shan, C. (2010). "A comparative study of HMMS and DBNS applied to facial action units recognition", *Neural Network World*, 20(6), 737-760.

[14] Swears E., Hoogs A., Ji Q. and Boyer, K. (2014). "Complex activity recognition using granger constrained DBN (GCDBN) in sports and surveillance video", *27th IEEE Conference on Computer Vision and Pattern Recognition*, 788-795.

[15] Faber M. H., Kroon I. B., Kragh E., Bayly D. and Decosemaeker P. (2002) "Risk assessment of decommissioning options using Bayesian networks", *Journal of Offshore Mechanics and Arctic Engineering*, 124(4), 231-238.

[16] Langseth H. and Portinale L. (2007). "Bayesian networks in reliability", *Reliability Engineering and System Safety*, 92(1), 92-108.

[17] Attoh-Okine N. O. and Bowers S. (2006). "A Bayesian belief network model of bridge deterioration", *Proceedings of the Institution of Civil Engineers: Bridge Engineering*, 159(2), 69-76.

[18] Palaniappan S. K., Akshay S., Liu B., Genest B. and Thiagarajan P. S. (2012). "Hybrid Factored Frontier Algorithm for Dynamic Bayesian Networks with a Biopathways Application", *IEEE-ACM Transactions on Computational Biology and Bioinformatics*, 9(5), 1352-1365.

[19] Doucet A., Godsill S. and Andrieu C. (2000). "On sequential Monte Carlo sampling methods for Bayesian filtering", *Statistics and Computing*, 10(3), 197-208.

[20] Arulampalam M. S., Maskell S., Gordon N. and Clapp T. (2002). "A tutorial on particle filters for online nonlinear/non-Gaussian Bayesian tracking", *IEEE Transactions on Signal Processing*, 50(2), 174-188.

[21] Langseth H. and Bangso O. (2001). "Parameter learning in object-oriented Bayesian networks", *Annals of Mathematics and Artificial Intelligence*, 32(1-4), 221-243.

[22] Shumway R. H. and Stoffer D. S. (1982). "An approach to time series smoothing and forecasting using the EM algorithm", *Journal of Time Series Analysis*, 3(4), 253-264.

[23] Vu K. A. T. and Stewart M. G. (2000). "Structural reliability of concrete bridges including improved chloride-induced corrosion models", *Structural Safety*, 22(4), 313-333.

[24] Stewart M. G. and Rosowsky D. V. (1998). "Time-dependent reliability of deteriorating reinforced concrete bridge decks", *Structural Safety*, 20(1), 91-109.

[25] Zhuhai Bureau of Transportation. (2013). "Zhuhai Transport Development Annual Report", Zhuhai.

[26] China highway planning and design institute. (2004). "General Code for Design of Highway Bridges and Culverts(JTG D60–2004)", *China Communications Press*, Beijing.

[27] China highway planning and design institute. (2004). "Code for design of highway reinforced concrete and prestressed concrete bridges and culverts(JTG D62-2004)", *China Communications Press*, Beijing.